Int J Clin Exp Pathol 2016;9(9):9058-9067
www.ijcep.com /ISSN:1936-2625/IJCEP0035121

Original Article

Blockade of IGFBPrP1 attenuates canine hepatic fibrosis induced by thioacetamide via inhibition of hepatic stellate cell activation

Yarong Guo[1], Haiyan Zhang[1,2,3], Qianqian Zhang[1,2,3], Xiaohong Guo[1,2,3], Lixin Liu[1,2,3]

[1]Department of Gastroenterology and Hepatology, [2]Experimental Center of Science and Research, The First Hospital of Shanxi Medical University, Taiyuan, Shanxi Province, China; [3]Key Laboratory of Cell Physiology, Provincial Department of The Ministry of Education, Shanxi Medical University, Taiyuan, Shanxi Province, China

Received July 5, 2016; Accepted August 20, 2016; Epub September 1, 2016; Published September 15, 2016

Abstract: Here we aimed to investigate the anti-fibrotic effect of the antibody against insulin-like growth factor binding protein-related protein 1 in a hepatic fibrosis canine model and explored the underlying mechanism. Advanced liver fibrosis was induced in beagles by thioacetamide administration for 12 weeks. From the 5th week, the animals received the antibody injections via the portal vein once a week. Liver biopsies were performed at weeks 0, 3, 6, 9, and 12. The pathological changes and fibrosis scores were examined. The dynamic changes in the expression of insulin-like growth factor binding protein-related protein 1, α-SMA, phosphorylation of the NF-κB subunit RelA at serine 536, and transforming growth factor β 1 during this process were studied using immunohistochemical methods. Hepatic insulin-like growth factor binding protein-related protein 1 expression significantly increased in the process of liver fibrosis from the 6th week and then sharply decreased from the 9th week due to blockade of insulin-like growth factor binding protein-related protein 1. In addition, the thioacetamide-induced liver fibrosis in the antibody-treated group was markedly attenuated as compared to that in the control group. Furthermore, the elevations in α-SMA, phosphorylation of the NF-κB subunit RelA at serine 536, and transforming growth factor β 1 levels in liver tissues were inhibited. Blockade of insulin-like growth factor binding protein-related protein 1 could ameliorate hepatic fibrosis in the canine model by inhibiting hepatic stellate cell activation and downregulating transforming growth factor β 1 via a mechanism involving the NF-κB pathway.

Keywords: IGFBPrP1, beagle dog, liver fibrosis, HSC, NF-κB, TGFβ1

Introduction

The burden of chronic hepatic disease is increasing and is becoming a cause for concern in China and worldwide. Progressive aggravation of chronic hepatic disease will inevitably trigger hepatic fibrosis [1]. However, to date, there is no established and licensed cure for liver fibrosis [2]. Therefore, the development of treatments that can promote the regression of advanced fibrosis would have crucial clinical impact. Hepatic fibrosis can be caused by excess deposition of extracellular matrix (ECM) proteins, especially collagen proteins, and most ECM components are produced by hepatic stellate cells (HSCs) [3].

Our previous findings have shown that exogenous insulin-like growth factor binding protein-related protein 1 (IGFBPrP1), a protein that is widely expressed in multiple tissues including the liver [4], can trigger the activation and transformation of HSCs and can further induce the expression of transforming growth factor β 1 (TGFβ1) [5, 6]. Furthermore, this process can be reversed via the blockade of IGFBPrP1 by IGFBPrP1-Ab in vitro and in mouse models [7]. Therefore, we speculated that IGFBPrP1 could be a potential anti-fibrotic target for clinical trials.

Nuclear factor-κB (NF)-κB regulates multiple essential functions in HSC, including the activation, survival, proliferation and apoptosis [8]. Usually, NF-κB activity is controlled by at least two key events during HSC activation. One is persistent repression of the IκB gene, which is modulated by epigenetic mechanism [9] and phosphorylation of the NF-κB subunit RelA at serine 536 (P-Ser^{536}-RelA) [10]. Moreover, the

inhibition of the RelA-Ser^{536} phosphorylation in fibrotic rodents can lead to the reduced survival of the activated HSC and fibrosis [11]. Recently, we showed that the NF-κB pathway is involved in the development of IGFBPrPl-induced hepatic fibrosis by using a PCR array [12]. However, whether IGFBPrPl-Ab promotes fibrosis regression through the NF-κB pathway is still unclear and the specific investigation of this aspect is needed.

Rodent models with multiple advantages have revolutionized our ability to understand human diseases. However, the average rate of final translation from lab findings in rodent models to practice in clinical trials is no more than 8% [13]. One of the major disadvantages of rodent models is that mice can bear higher drug levels than humans [14]. Given the big species-level differences between mice and humans, the use of other animal models, such as canine models, becomes important. Besides, the similarity in the anatomy, physiology, genome, molecular mechanisms of liver fibrosis, and response to cytotoxic agents between canine models and humans is higher than that between rodent models and humans [15, 16]. Therefore, we believed that the use of canine models in our hepatic fibrosis study would be more suitable to acquire more deducible and referenced data that can be used in further clinical research.

Thioacetamide (TAA) is a well-known hepatotoxic agent. The pathology of a rodent model of hepatic fibrosis established using TAA most closely resembled that observed in human patients with alcoholic liver fibrosis [17] and liver fibrosis caused by viral infection [18]. Therefore, in this study, we used TAA to establish a canine model of hepatic fibrosis and observed the different stages of TAA-induced liver fibrosis in beagles. The main aim of this study was to determine the effects of IGFBPrP1 inhibition established using anti-IGFBPrP1 antibody on hepatic fibrosis and to elucidate the mechanisms underlying this effect. Given the similarities between canine models and humans in the context of liver fibrosis, we believe that our findings will be of significance for future research on liver fibrosis in humans.

Materials and methods

Establishment of the canine model

Healthy 8-month-old male beagles of weighing between 7.5 and 8.0 kg were purchased from the Beijing Rixin Technology Company (SCXK [Beijing] 2011-0007; China). The beagles were maintained in the laboratory of the Chinese Institute for Radiation Protection (SYXK [Shanxi] 2013-0002; China).

The beagles were divided into five groups (n=6): (i) control beagles receiving normal saline; (ii) negative control beagles receiving 5 μg IgG antibody/kg body weight (RD AB-105-C); (iii) TAA (Sigma, St Louis, MO, USA)-injected beagles (injected with 12 mg TAA/kg body weight, twice a week) receiving normal saline; (iv) TAA-injected beagles receiving 5 μg anti-IGFBPrP1 antibody/kg body weight (Abcam, Cambridge, UK); and (v) TAA-injected beagles receiving 28 mg silibinin/kg body weight (kindly provided by TASLY PHARM Company, Tianjing, China). The antibody was delivered via the portal vein once weekly during the last 8 weeks of the 12 weeks of TAA administration. Simultaneously, silibinin was administered by gavage once a day for 8 weeks. Before the antibody was injected, the portal delivery system was introduced as described in a previous report [19].

Liver biopsy

All the beagles underwent liver biopsy at weeks 0, 3, 6, 9, and 12 under anesthesia. The liver biopsies were obtained using a 14G Precisa needle under ultrasound guidance [20]. The biopsies were pathologically evaluated, and hepatic fibrosis score was determined according to the Metavir scoring system [21].

Histology and immunohistochemistry

Hematoxylin and eosin (H&E) staining, Masson's trichrome staining and immunohistochemical staining were performed as described in our previous report [6].

Confocal microscopy

Immunofluorescence staining was performed to examine the expression of IGFBPrP1 and α-smooth muscle actin (α-SMA) in the livers of the beagles. Briefly, the tissue slides were fixed in acetone, permeabilized with 0.3% Triton X-100 (Sigma), and blocked with 3% bovine serum albumin (Sigma), followed by incubation with anti-IGFBPrP1 (1:200; Abcam, Cambridge, UK) and anti-α-SMA (1:50; Abcam, United Kingdom) primary antibodies at 4°C overnight. After

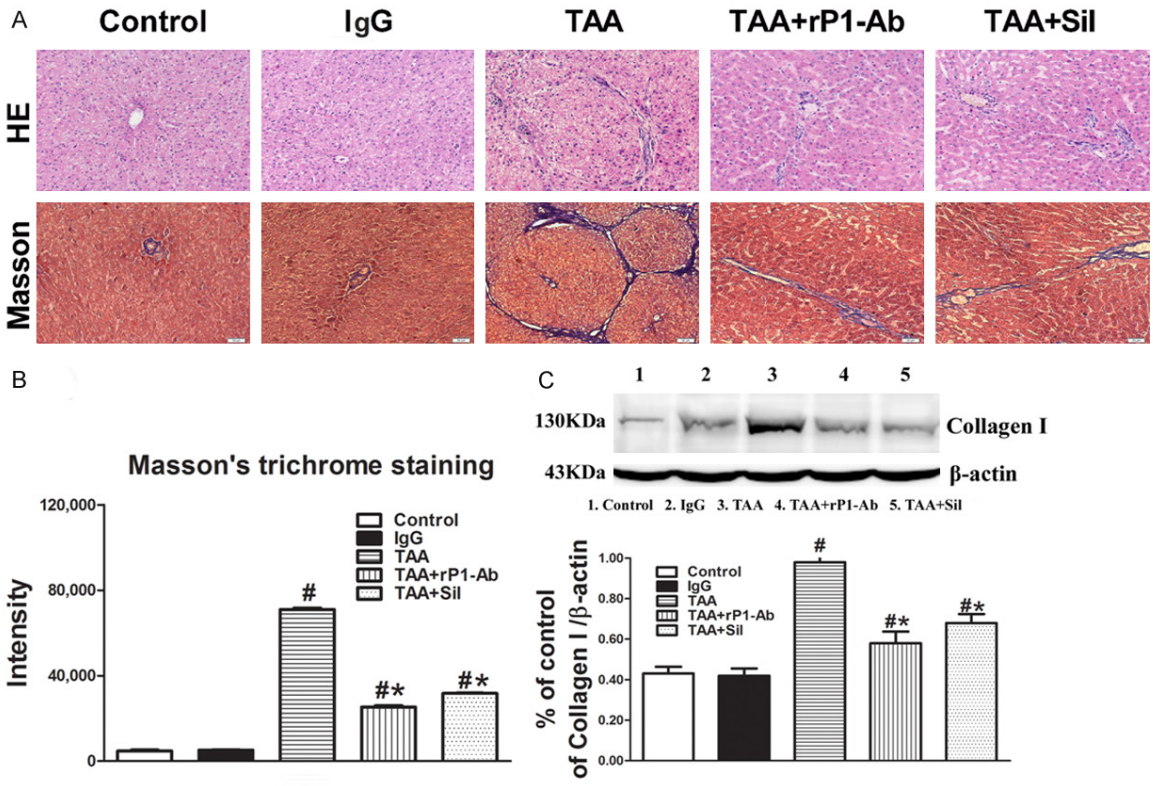

Figure 1. Blockade of IGFBPrP1 by IGFBPrP1-Ab attenuated TAA-induced liver fibrosis in beagles at week 12. A: Histological analysis after hematoxylin and eosin and Masson's trichrome staining showed cirrhosis in the TAA group. Treatment with IGFBPrP1-Ab (TAA+rP1-Ab) or silibinin (TAA+Sil) partly reversed the liver fibrosis induced by TAA (magnification 200×). B: Semi-quantitative analysis of liver sections. C: IGFBPrP1-Ab or silibinin treatment reduced the protein expression of Collagen I, as determined using western blotting. The results were quantified by densitometry. The number of beagles in each group is 6. Each graphic represents the mean values (± SD) of three experiments. $^{\#}P < 0.05$ vs. control group and IgG group; $^{*}P < 0.05$ vs. TAA group.

three washes with PBS containing 0.1% Tween-20 (PBST), the slides were incubated with secondary Cy3-conjugated antibodies (1:60; Boster, China) and FITC-conjugated antibodies (1:100; Santa Cruz Biotechnology, CA, USA) for 1 h at 37°C. The slides were again washed three times with PBS containing 0.1% Tween-20 (PBST), and DAPI (4, 6-diamidine-2-phenylindole dihydrochloride) (1 μg/mL; Roche) was then used to stain the nuclei. The tissues were observed and imaged using a FV1000 OLYMPUS scanning confocal microscope (OLYMPUS, Japan).

Western blot analysis

Equal amounts of the protein (20 μg/lane) were separated by SDS-PAGE and transferred to PVDF membranes (Bio-Rad Laboratories, Hercules, CA, USA). The membranes were then probed with anti-α-SMA and anti-IGFBPrP1 (Abcam, Cambridge, UK), anti-Collagen I (Santa Cruz Biotechnology, CA, USA), and anti-TGFβ1 (Sangon Biotechnology, Shanghai, China) antibodies. Immunodetection was conducted using the ECL detection system (ECL; Bio-Rad Laboratories, Hercules, CA, USA) according to the manufacturer's instructions. Quantitative densitometric analyses of the immunoblot images were performed using Bio-Rad Quantity One software.

Statistical analysis

The mean and standard deviation were calculated for all the measurements. Statistical significance was estimated using one-way analysis of variance (ANOVA), repeated-measures analysis of variance, or Wilcoxon's Sign Rank Test. In addition, the Pearson correlation coefficients (r-values) were calculated. The level of statistical significance was set as $P < 0.05$.

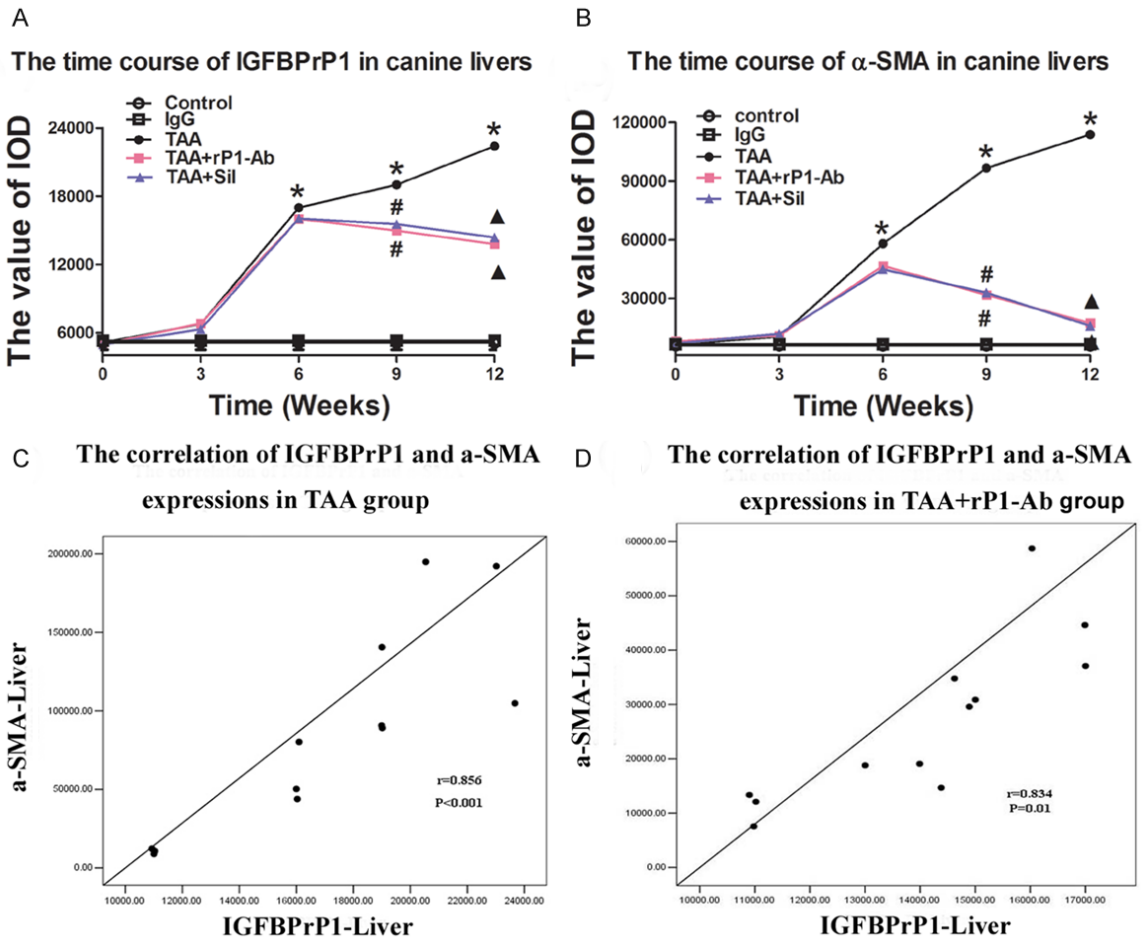

Figure 2. IGFBPrP1-Ab decreased IGFBPrP1 protein expression in the livers injected with TAA and inhibited HSC activation. Liver samples of each animal were collected at weeks 0, 3, 6, 9 and 12 after TAA injection. IGFBPrP1 and α-SMA expression in the liver tissues of beagles treated with saline, IgG, TAA plus saline, rP1-Ab, or Sil were assessed by immunohistochemical staining. (A) IGFBPrP1 level in the liver tissues. (B) α-SMA level in the liver tissues of the five groups. Values are expressed as the mean ± SD. $^{*}P < 0.05$ vs. control group, IgG group, and TAA group at 0 weeks, $^{\#}P < 0.05$ vs. the TAA group at 9 weeks, $^{\blacktriangle}P < 0.05$ vs. the TAA group at 12 weeks. Relationship between the expression of IGFBPrP1 and α-SMA at multiple time points in the canine model (C) or in the TAA+rP1-Ab group (D).

Results

Histological examination

We used TAA at doses of 10, 20, and 40 mg/kg body weight to induce hepatic fibrosis in the beagles; administration of TAA at 10 mg/kg did not result in significant hepatic fibrosis, and the latter two doses were too high and resulted in an increased rate of mortality, reflecting severe hepatotoxicity. Finally, the hepatic-fibrosis model was successfully established through TAA administration twice a week for 12 weeks, which was confirmed using Metavir scores. As shown in Table S1, the pathological examination of the liver biopsies (n=30) obtained from the TAA group at weeks 0, 3, 6, 9, and 12 revealed that different stages of liver fibrosis had been successfully established in the 6 beagles. After 3 weeks of TAA administration, compared with the control, the TAA-treated groups showed a gradual increase in hepatocyte degeneration and inflammatory cell infiltration in the portal area. At 6 weeks, the formation of fibrous septum could be observed in the liver. At week 12, pseudolobuli could be seen in some canine livers (Metavir F3-4) (Figure S1). Meanwhile, the lobular structure was maintained and no nodules were found in the specimen of TAA+rP1-Ab group and TAA+Sil group (**Figure 1A**). Moreover, the scores for TAA-induced hepatic fibrosis were significantly

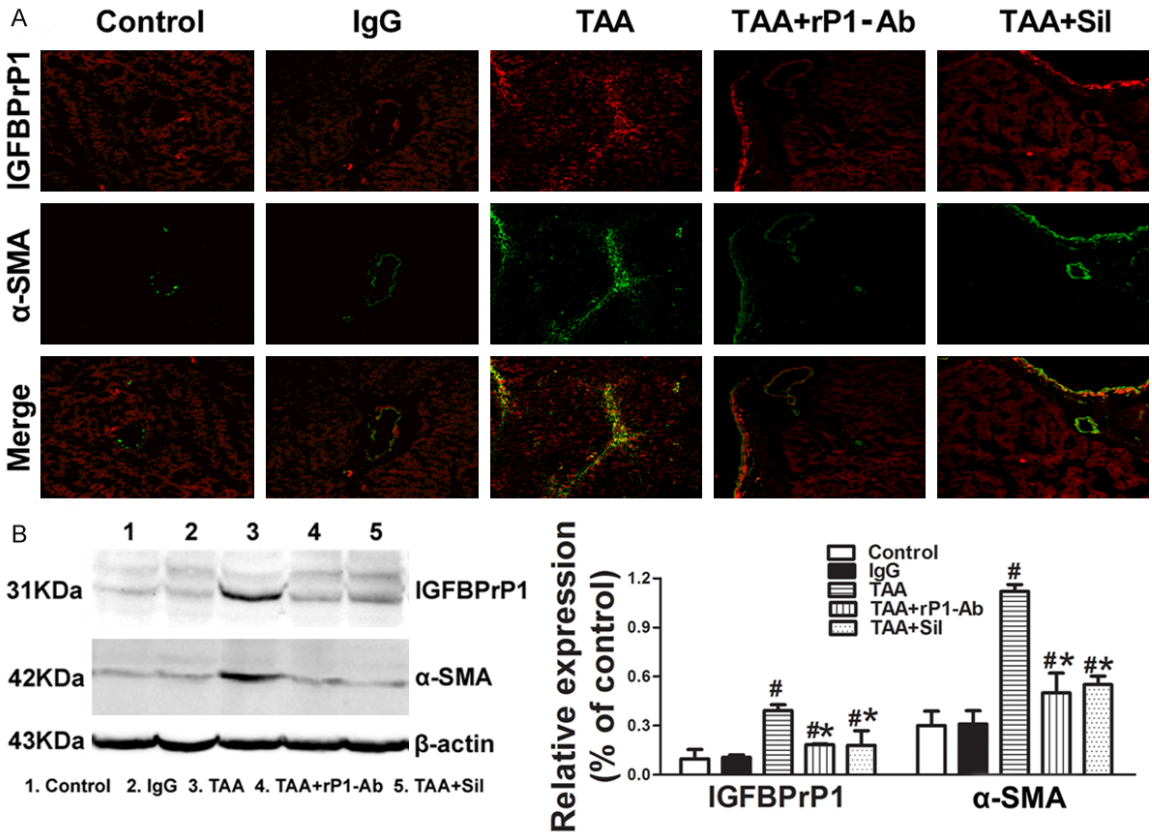

Figure 3. At week 12 after TAA injection, IGFBPrP1 blockade enabled IGFBPrP1 inhibition in the myofibroblasts. A: Immunofluorescence staining for IGFBPrP1 (red) and α-SMA (green) was performed using frozen liver sections (magnification 200×). Double-positive cells were observed in the myofibroblasts and in the fibrosis area. The images for fluorescein-isothiocyanate and rhodamine staining were overlayed using OLYMPUS image analysis software. B: Analysis of hepatic IGFBPrP1 and α-SMA expression by western blot, and the relative protein levels measured using Bio-Rad Quantity One software. Histograms represent mean ± SD (n=6). #$P < 0.05$ vs. control group and IgG group; *$P < 0.05$ vs. TAA group.

reduced after IGFBPrP1-Ab or silibinin treatment (Metavir F1-2) (Table S2; $P < 0.001$). Quantification of the results of Masson's trichrome staining showed an 8-fold higher collagen accumulation in the fibrotic beagles compared to that in the control and IgG groups, while the administration of IGFBPrP1-Ab resulted in a 45% reduction in staining (**Figure 1B**).

Hepatic collagen content

At week 12, TAA administration significantly increased the expression of Collagen I protein, as determined using western blot in the whole liver lysates (0.98±0.053 vs. 0.43±0.034, $P < 0.001$); however, collagen I protein expression decreased after IGFBPrP1-Ab or silibinin treatment (0.58±0.057 vs. 0.98±0.053 and 0.68±0.044 vs. 0.98±0.053, respectively, $P < 0.001$) (**Figure 1C**).

Expression levels of IGFBPrP1, α-SMA and P-Ser^{536}-RelA proteins at multiple time points in the beagle livers

The dynamic expression of IGFBPrP1 and α-SMA, as determined using immunohistochemical staining, gradually increased in the beagles post-TAA administration compared to the baseline values at weeks 6, 9 and 12 (**Figure 2A**, **2B**) ($P < 0.05$). The dynamic expression of IGFBPrP1 significantly decreased from the 9th week in the TAA+rP1-Ab and TAA+Sil groups as compared to the TAA group (1.50±0.01 vs. 1.90±0.01, ×10^4 and 1.55±0.01 vs. 1.90±0.01, ×10^4, respectively, $P < 0.05$) (**Figure 2A**). However, α-SMA expression was maintained at a constantly high level until week 9 (3.17±0.27 vs. 9.67±2.93, ×10^4 and 3.30±1.10 vs. 9.67±2.93, ×10^4, respectively, $P < 0.05$) (**Figure 2B**). The IGFBPrP1 levels show-

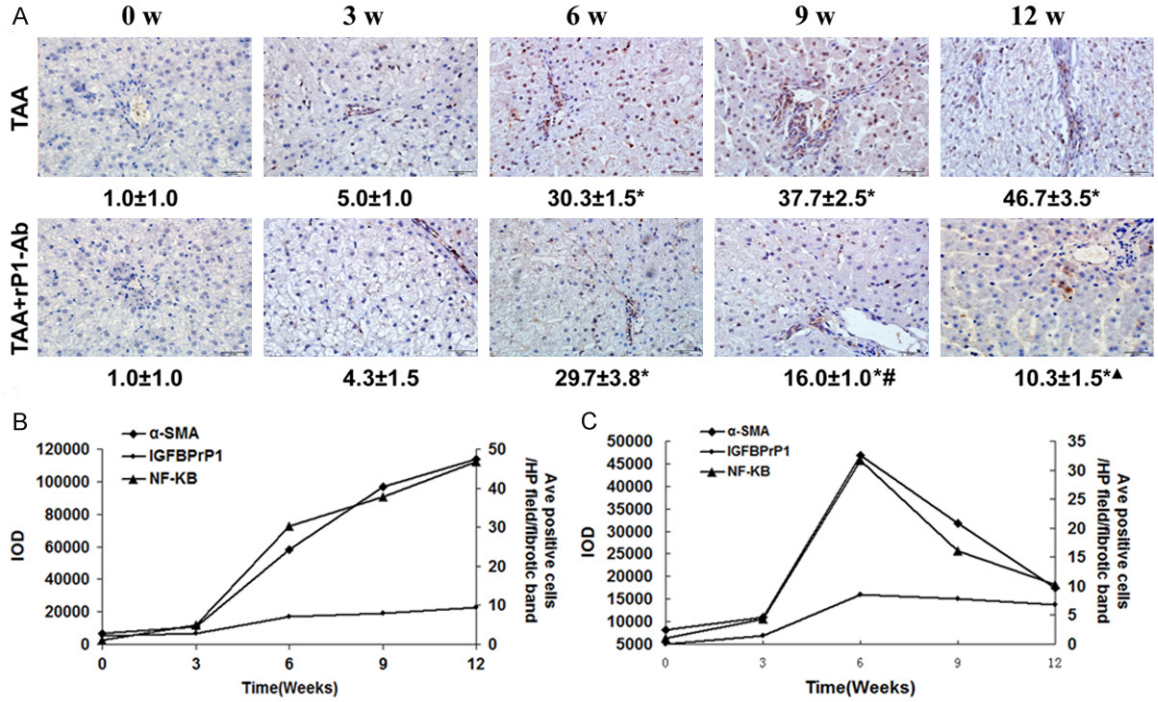

Figure 4. IGFBPrP1 blockade gradually inhibits the phosphorylation of Ser^{536}-RelA in the HSCs of beagles with established fibrosis. (A) Photomicrographs (magnification 400×) show liver sections without (top) or with IGFBPrP1-Ab treatment (bottom), immunostained with anti-P-Ser^{536}-RelA antibodies. Cell counts show the average number of positively stained cells in the fibrotic bands of the canine liver biopsy specimens, expressed as mean ± SD (n=6). *P < 0.05 vs. control group, IgG group, and TAA group at 0 weeks, $^{\#}P$ < 0.05 vs. TAA group at 9 weeks, $^{\blacktriangle}P$ < 0.05 vs. TAA group at 12 weeks. The dynamic expression of IGFBPrP1, α-SMA, and P-Ser^{536}-RelA in the liver tissues of the control group (B) and TAA+rP1-Ab group (C).

ed a positive correlation with α-SMA expression in the TAA and TAA+rP1-Ab groups (r= 0.856, P < 0.001; r=0.834, P=0.01, respectively) (**Figure 2C**, **2D**).

Figure 3A shows the expression of IGFBPrP1 and α-SMA, as determined using immunofluorescence staining. IGFBPrP1 and α-SMA were mainly colocalized in the activated HSCs and in the fibrous area after TAA treatment at week 12. Quantitative analysis of both IGFBPrP1-positive cells and myofibroblastic cells showed that the values of Integral optical density (IOD) in the TAA group were significantly higher (data not shown) than those in the saline-treated beagles (1.10±0.01 vs. 0.38±0.03, ×10^5 and 0.69±0.04 vs. 0.05±0.01, ×10^5, respectively P < 0.05). In addition, the number of IGFBPrP1 and α-SMA double-positive cells was significantly reduced upon treatment with IGFBPrP1-Ab or silibinin.

Western blot analysis revealed that the levels of IGFBPrP1 and α-SMA proteins were up-regulated in the model group at week 12. In contrast, with the blockade of IGFBPrP1, the expression of both IGFBPrP1 and α-SMA was significantly downregulated at the same time (0.18±0.01 vs. 0.39±0.02 and 0.21±0.01 vs. 0.52±0.02, respectively, P < 0.05 as compared to the TAA group) (**Figure 3B**). In addition, silibinin treatment significantly decreased the hepatic protein expressions of IGFBPrP1 and α-SMA in the TAA group.

Compared with the baseline values 0 week, the number of P-Ser^{536}-RelA-positive cells in the fibrotic band significantly (P < 0.05) increased in the beagles post-TAA injection at weeks 6, 9, and 12 (**Figure 4A**). Staining of the liver biopsy slides for P-Ser^{536}-RelA indicated that the beagles that underwent regression from the 9th week in the TAA+rP1-Ab groups showed a lower number of P-Ser^{536}-RelA-positive cells than the TAA group (**Figure 4A**).

In summary, the dynamic expression of IGFBPrP1, α-SMA, and P-Ser^{536}-RelA reached a max-

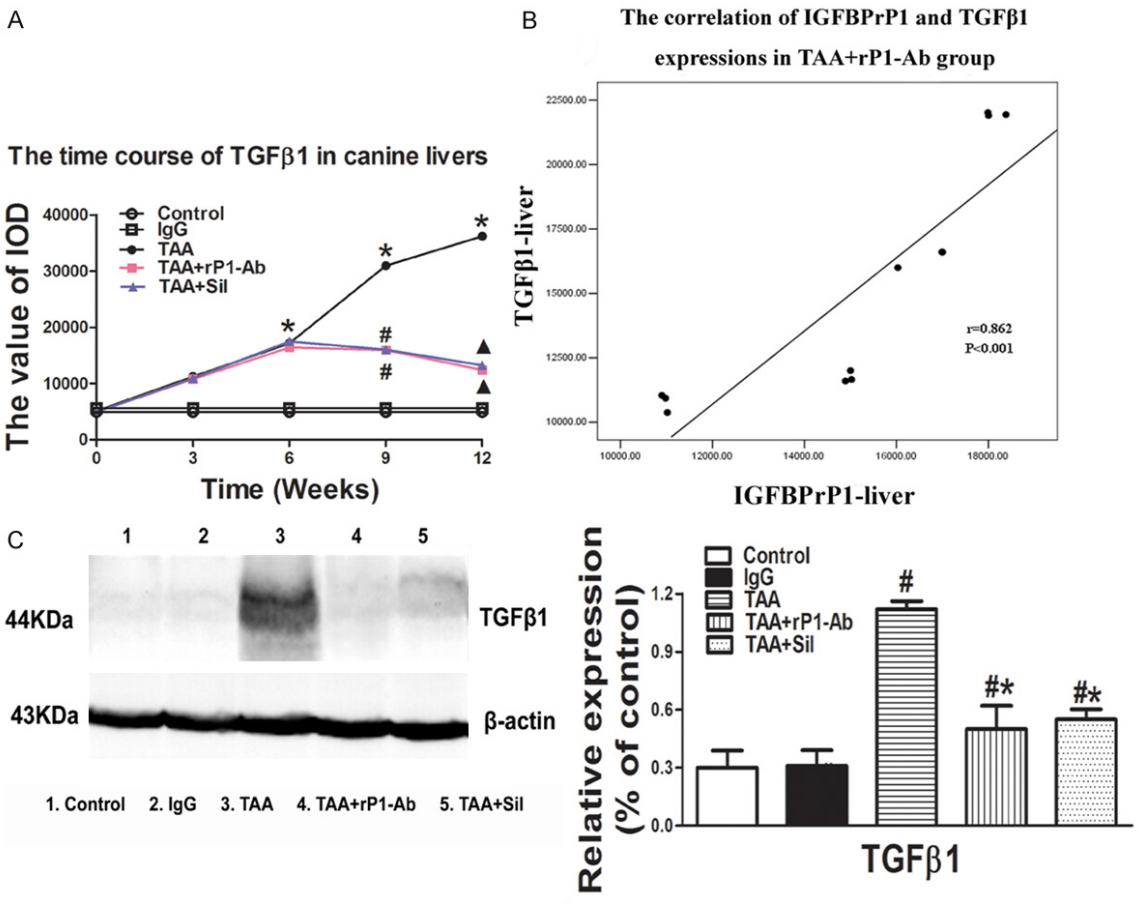

Figure 5. IGFBPrP1-Ab was involved in the downregulation of TGFβ1 in the liver tissue. A: Livers from beagles treated with saline, IgG, TAA plus saline, rP1-Ab, or Sil for 0, 3, 6, 9 and 12 weeks were analyzed for TGFβ1 levels using immunohistochemical staining. Data are expressed as mean ± SD (n=6). $^{*}P < 0.05$ vs. control group, IgG group, and TAA group at 0 weeks, $^{\#}P < 0.05$ vs. TAA group at 9 weeks, $^{\blacktriangle}P < 0.05$ vs. TAA group at 12 weeks. B: Correlation analysis of the IGFBPrP1 and TGFβ1 protein levels in the TAA+rP1-Ab group. C: IGFBPrP1-Ab or silibinin treatment decreased hepatic TGFβ1 protein expression in the TAA-injected beagles, as determined using western blot at week 12. $^{\#}P < 0.05$ vs. control group and IgG group; $^{*}P < 0.05$ vs. TAA group.

imum at week 12 in the TAA group (**Figure 4B**) and at week 6 in the TAA+rP1-Ab group (**Figure 4C**).

Effect of IGFBPrP1 on dynamic expression of TGFβ1 in the livers of the TAA-treated beagles

The expression of TGFβ1, the main cytokine involved in liver fibrogenesis, significantly increased in the beagles post-TAA administration compared to the baseline values from the 6th week, as determined by immunohistochemical staining ($P < 0.05$). On the other hand, the dynamic expression of TGFβ1 significantly decreased at weeks 9 and 12 in the TAA+rP1-Ab and TAA+Sil groups compared with those in the TAA group ($P < 0.05$) (**Figure 5A**). Moreover, there was a statistically significant positive correlation between TGFβ1 and IGFBPrP1 expression in the TAA+rP1-Ab group (**Figure 5B**).

At week 12, the TGFβ1 protein level observed in the immunoblots (**Figure 5C**) was consistent with the results of the immunohistochemical staining.

Discussion

In this study, we observed the dynamic changes in hepatic histopathology in beagles using liver biopsy specimens obtained under ultrasound guidance. First, we demonstrated the successful establishment of a canine model of

hepatic fibrosis using TAA. The optimal dose of TAA was determined as 12 mg/kg based on our previous results in mice [7]. Our findings indicate that IGFBPrP1 blockade attenuated the TAA-induced hepatic fibrosis in the beagles via inhibition of HSC activation.

Despite the relatively invasive nature of biopsy procedures, percutaneous liver biopsy is still acknowledged globally as the "gold standard" of hepatic-histopathological assessment for its accuracy [22]. Usually, dynamic diagnosis of experimental liver injuries in rats or mice is conducted via execution of the animals at multiple time points. However, liver biopsy could be operated on dogs repeatedly, and few complications have been recorded during the course [23]. Therefore, we used liver biopsy samples from the beagles to evaluate the successful establishment of the canine hepatic fibrosis model and for the subsequent experiments in our study.

IGFBPrP1 is highly expressed in activated human HSC and HSC-T6 cell lines, as well as in fibrotic and cirrhotic human liver specimens [7, 24, 25]. To investigate the relationship of IGFBPrP1 expression with HSC activation in our canine model, we observed the dynamic change in IGFBPrP1 expression using immunohistochemical staining and performed immunofluorescent staining of the liver biopsy specimens for IGFBPrP1 and α-SMA (a marker for activated HSCs). The expression of IGFBPrP1 and α-SMA in the TAA-treated beagles showed a marked increase with time (**Figure 2**). The IGFBPrP1 level also showed a positive correlation with α-SMA levels ($r=0.856$, $P < 0.001$). IGFBPrP1 and α-SMA double-positive cells were colocalized in the activated HSCs and in the fibrous area, and their numbers were significantly increased in the TAA-treated beagles (**Figure 3**). This result indicated that IGFBPrP1 secretion in the TAA-treated beagles could be induced HSC activation. Together with the results of our previous studies [5, 6], this result suggests that HSC activation can be induced by IGFBPrP1 both in vitro and in vivo, which indicates a critical role for IGFBPrP1 in the mechanisms of HSC activation. Therefore, we hypothesize the existence of a positive feedback cycle in which IGFBPrP1 and HSCs stimulate each other.

HSCs are now widely acknowledged as the prominent effector [26]. NF-κB is constitutively active during this course [27]. Constitutively active NF-κB containing the P-Ser^{536}-RelA subunit is expressed in both cultured HSCs and myofibroblasts of diseased human livers, which is a characteristic feature of these cells [10]. In this study, we found that the number of scar-associated P-Ser^{536}-RelA-positive cells gradually increased with the development of hepatic fibrosis. The increase in the number of these cells was found to be correlated with the elevation of α-SMA expression in the diseased beagle livers treated with TAA ($r=0.971$, $P < 0.001$), indicating that RelA at Ser536 may mediate HSC activation in this hepatic fibrosis model induced by TAA administration.

To further determine the effect of IGFBPrP1 on liver fibrogenesis, IGFBPrP1-Ab was administered via the portal vein weekly for 8 weeks in this canine model. Our findings showed that the elevations in IGFBPrP1 levels in the liver significantly decreased at weeks 9 and 12 in the TAA+rP1-Ab group compared to those in the TAA group (**Figure 2A**). Given that portal vein injection delivers vectors efficiently and directly into the liver of beagles [19], our results indicated that IGFBPrP1-Ab entered the canine liver and blocked IGFBPrP1 in the sinusoid attenuated hepatic fibrosis, as assessed by the decreased collagen deposition and less advanced stage of fibrosis observed.

A single stellate cell usually surrounds more than two nearby sinusoids, where the HSCs can interact with soluble medium [28]. After the blockade of IGFBPrP1 in the sinusoid, the number of activated HSCs was markedly reduced from the 9th week (**Figure 2B**). Moreover, we observed P-Ser^{536}-RelA positivity in the livers of the hepatic fibrosis beagles, which followed a similar trend as the α-SMA staining (**Figure 4**). Resolution of fibrosis induces pathways that either drive the HSCs toward apoptosis or promote their reversion to a quiescent phenotype [27]. It has been reported that IGFBPrP1-Ab can effectively reverse the activation of HSC-T6 cells [5]. In addition, P-Ser^{536}-RelA may be a core regulator of the activation of human and rodent hepatic HSC [10]. During the resolution of hepatic fibrosis in our study models, decreased IGFBPrP1 expression was associated with a reduced number of α-SMA-positive HSCs, which presumably occurred

through the inhibition of RelA-Ser^{536} phosphorylation.

TGFβ1 is a multifunctional cytokine with well-known profibrotic properties [29]. Accumulated evidences have indicated that IGFBPrP1 can strongly stimulate TGFβ1 expression in P69 and Hs578T cells [30]. Moreover, our previous study suggested that IGFBPrP1 acts as an upstream activator of TGFβ1 both in a fibrotic rodent model and under in vitro conditions [6, 7]. In the present study, we found that IGFBPrP1-Ab treatment significantly inhibited the elevations of TGFβ1 levels in the liver tissue compared to those in the TAA group, which followed a pattern similar to that of P-Ser^{536}-RelA expression (r=0.876, $P < 0.01$) (Figure S2). Furthermore, mRNA transcription of TGFβ1 could be regulated by the NF-κB signaling pathway in HSCs [31]. Based on our findings and analyses described above, we believe that the blockade of IGFBPrP1 in the TAA-treated beagles may affect the expression of TGFβ1 in these animals and that this effect could be involved in the antifibrotic effects observed.

In addition, silibinin (a major constituent of the milk thistle) has been used for two millennia to treat various liver disorders. There are substantial evidences suggesting that silibinin exerts antifibrotic effects in rodent animal models [32]. However, the underlying mechanisms remain unclear. We found that down-regulation of hepatic IGFBPrP1 protein expression in TAA-injected beagles was partially corrected by silibinin treatment (**Figure 2A**). Thus, IGFBPrP1 may be the novel target for silibinin and silibinin attenuates hepatic fibrosis. However, more studies will be needed to confirm this aspect.

Conclusion

We successfully established a reliable canine model of liver fibrosis induced by TAA. The results indicated that IGFBPrP1 plays a crucial role in liver fibrogenesis and that treatment with IGFBPrP1-Ab or silibinin can efficiently inhibit IGFBPrP1 expression and prevent fibrogenesis in this model. In addition, downregulation of hepatic IGFBPrP1 expression might be involved in the reduction of HSC activation and suppression of TGFβ1 expression in the canine liver fibrosis model. These results suggest that the molecular mechanism of this phenomenon may be associated with the NF-κB pathway.

Acknowledgements

This study was funded by National Natural Science Foundation of China (No 81141049) and Shanxi Provincial Key Scientific Research Project for the Returned Scholars (2012-4). We are grateful for the native language-polishing help from Roy Fyre, who is an Associate Professor at the department of pathology at the University of Pittsburgh.

Disclosure of conflict of interest

None.

Address correspondence to: Dr. Lixin Liu, Department of Gastroenterology and Hepatology, The First Hospital of Shanxi Medical University, Mailbox 427, 85 South Jiefang Road, Taiyuan 030001, Shanxi Province, China. Tel: +86-351-4639075; Fax: +86-351-8263169; E-mail: lixinliu6@hotmail.com

References

[1] Ahmad A, Ahmad R. Understanding the mechanism of hepatic fibrosis and potential therapeutic approaches. Saudi J Gastroenterol 2012; 18: 155-167.

[2] Sohrabpour AA, Mohamadnejad M, Malekzadeh R. Review article: the reversibility of cirrhosis. Aliment Pharmacol Ther 2012; 36: 824-832.

[3] Friedman SL. Evolving challenges in hepatic fibrosis. Nat Rev Gastroenterol Hepatol 2010; 7: 425-436.

[4] Chen D, Siddiq A, Emdad L, Rajasekaran D, Gredler R, Shen XN, Santhekadur PK, Srivastava J, Robertson CL, Dmitriev I, Kashentseva EA, Curiel DT, Fisher PB, Sarkar D. Insulin-like growth factor-binding protein-7 (IGFBP7): a promising gene therapeutic for hepatocellular carcinoma (HCC). Mol Ther 2013; 21: 758-766.

[5] Liu LX, Huang S, Zhang QQ, Liu Y, Zhang DM, Guo XH, Han DW. Insulin-like growth factor binding protein-7 induces activation and transdifferentiation of hepatic stellate cells in vitro. World J Gastroenterol 2009; 15: 3246-3253.

[6] Guo YR, Zhang Y, Zhang QQ, Guo X, Zhang H, Zheng G, Liu L. Insulin-like growth factor binding protein-related protein 1 (IGFBPrP1) contributes to liver inflammation and fibrosis via activation of the ERK1/2 pathway. Hepatol Int 2015; 9: 130-141.

[7] Liu LX, Zhang HY, Zhang QQ, Guo XH. Effects of insulin-like growth factor binding protein-related protein 1 in mice with hepatic fibrosis induced by thioacetamide. Chin Med J (Engl) 2010; 123: 2521-2526.
[8] Luedde T, Schwabe RF. NF-κB in the liver-linking injury, fibrosis and hepatocellular carcinoma. Nat Rev Gastroenterol Hepatol 2011; 8: 108-118.
[9] Mann J, Oakley F, Akiboye F, Elsharkawy A, Thorne AW, Mann DA. Regulation of myofibroblast transdifferentiation by DNA methylation and MeCP2: implications for wound healing and fibrogenesis. Cell Death Differ 2007; 14: 275-285.
[10] Oakley F, Teoh V, Ching ASG, Bataller R, Colmenero J, Jonsson JR, Eliopoulos AG, Watson MR, Manas D, Mann DA. Angiotensin II activates I kappaB kinase phosphorylation of RelA at Ser 536 to promote myofibroblast survival and liver fibrosis. Gastroenterol 2009; 136: 2334-2344.
[11] Moles A, Sanchez AM, Banks PS, Murphy LB, Luli S, Borthwick L, Fisher A, O'Reilly S, van Laar JM, White SA, Perkins ND, Burt AD, Mann DA, Oakley F. Inhibition of RelA-Ser536 phosphorylation by competing peptide reduces mouse liver fibrosis without blocking the innate immune response. Hepatology 2013; 57: 817-828.
[12] Guo X, Zhang H, Zhang Q, Li X, Liu L. Screening for and validation of a hepatic fibrosis-related pathway induced by insulin-like growth factor-binding protein-related protein 1. Eur J Gastroenterol Hepatol 2016; 28: 762-772.
[13] Cekanova M, Rathore K. Animal models and therapeutic molecular targets of cancer: utility and limitations. Drug Des Devel Ther 2014; 8: 1911-1921.
[14] Mak IW, Evaniew N, Ghert M. Lost in translation: animal models and clinical trials in cancer treatment. Am J Transl Res 2014; 6: 114-118.
[15] Paoloni M, Khanna C. Translation of new cancer treatments from pet dogs to humans. Nat Rev Cancer 2008; 8: 147-156.
[16] Kanemoto H, Ohno K, Sakai M, Nakashima K, Takahashi M, Fujino Y, Tsujimoto H. Expression of fibrosis-related genes in canine chronic hepatitis. Vet Pathol 2011; 48: 839-845.
[17] Lv J, Nie ZK, Zhang JL, Liu FY, Wang ZZ, Ma ZL, He H. Corn peptides protect against thioacetamide-induced hepatic fibrosis in rats. J Med Food 2013; 16: 912-919.
[18] Salguero Palacios R, Roderfeld M, Hemmann S, Rath T, Atanasova S, Tschuschner A, Gressner OA, Weiskirchen R, Graf J, Roeb E. Activation of hepatic stellate cells is associated with cytokine expression in thioacetamide-induced hepaticfibrosis in mice. Lab Invest 2008; 88: 1192-1203.
[19] Sherman A, Schlachterman A, Cooper M, Mericks EP, Raymer RA, Bellinger DA, Herzog RW, Nichols TC. Portal vein delivery of viral vectors for gene therapy for hemophilia. Methods Mol Biol 2014; 1114: 413-426.
[20] Hoffmann G, van den Ingh TS, Bode P, Rothuizen J. Copper-associated chronic hepatitis in Labrador Retrievers. J Vet Intern Med 2006; 20: 856-861.
[21] Bedossa P, Poynard T. An algorithm for the grading of activity in chronic hepatitis C. The METAVIR Cooperative Study Group. Hepatology 1996; 24: 289-293.
[22] Toosi AE. Liver Fibrosis: Causes and Methods of Assessment, A Review. Rom J Intern Med 2015; 53: 304-314.
[23] Barr F. Percutaneous biopsy of abdominal organs under ultrasound guidance. J Small Anim Pract 1995; 36: 105-113.
[24] Guo XH, Liu LX, Zhang HY, Zhang QQ, Li Y, Tian XX, Qiu ZH. Insulin-like growth factor binding protein-related protein 1 contributes to hepatic fibrogenesis. J Dig Dis 2014; 15: 202-210.
[25] Boers W, Aarrass S, Linthorst C, Pinzani M, Elferink RO, Bosma P. Transcriptional Profiling Reveals Novel Markers of Liver Fibrogenesis. J Biol Chem 2006; 281: 16289-16295.
[26] Reeves HL, Friedman SL. Activation of hepatic stellate cells-a key issue in liver fibrosis. Front Biosci 2002; 7: d808-d826.
[27] Mann DA, Smart DE. Transcriptional regulation of hepatic stellate cell activation. Gut 2002; 50: 891-896.
[28] Wake K. Hepatic stellate cells: Three-dimensional structure, localization, heterogeneity and development. Proc Jpn Acad Ser B Phys Biol Sci 2006; 82: 155-164.
[29] Weiskirchen R. Hepatoprotective and Antifibrotic Agents: It's Time to Take the Next Step. Front Pharmacol 2016; 6: 303.
[30] Hwa V, Tomasini-Sprenger C, Bermejo AL, Rosenfeld RG, Plymate SR. Characterization of insulin-like growth factor-binding protein-related protein-1 in prostate cells. J Clin Endocrinol Metab 1998; 83: 4355-4362.
[31] Cui D, Zhang S, Ma J, Han J, Jiang H. Short interfering RNA targetting NF-kappa B induces apoptosis of hepatic stellate cells and attenuates extracellular matrix production. Dig Liver Dis 2010; 42: 813-817.
[32] Clichici S, Olteanu D, Nagy AL, Oros A, Filip A, Mircea PA. J Med Food 2015; 18: 290-298.

Table S1. Pathological staging of liver biopsies from dogs in the TAA group at several time points

Time	F0	F1	F2	F3	F4	Median
0 w	6	0	0	0	0	0
3 w	5	1	0	0	0	0 (0, 0.25)
6 w	0	4	2	0	0	1 (1, 2)[a,b]
9 w	0	0	1	5	0	3 (2.75, 3)[a,b,c]
12 w	0	0	0	3	3	3.5 (3, 4)[a,b,c]

Data are presented as the median (min.-max.). Note: [a]$P < 0.05$ vs. the TAA group at 0 weeks; [b]$P < 0.05$ vs. the TAA group at 3 weeks; [c]$P < 0.05$ vs. the TAA groups at 6 weeks.

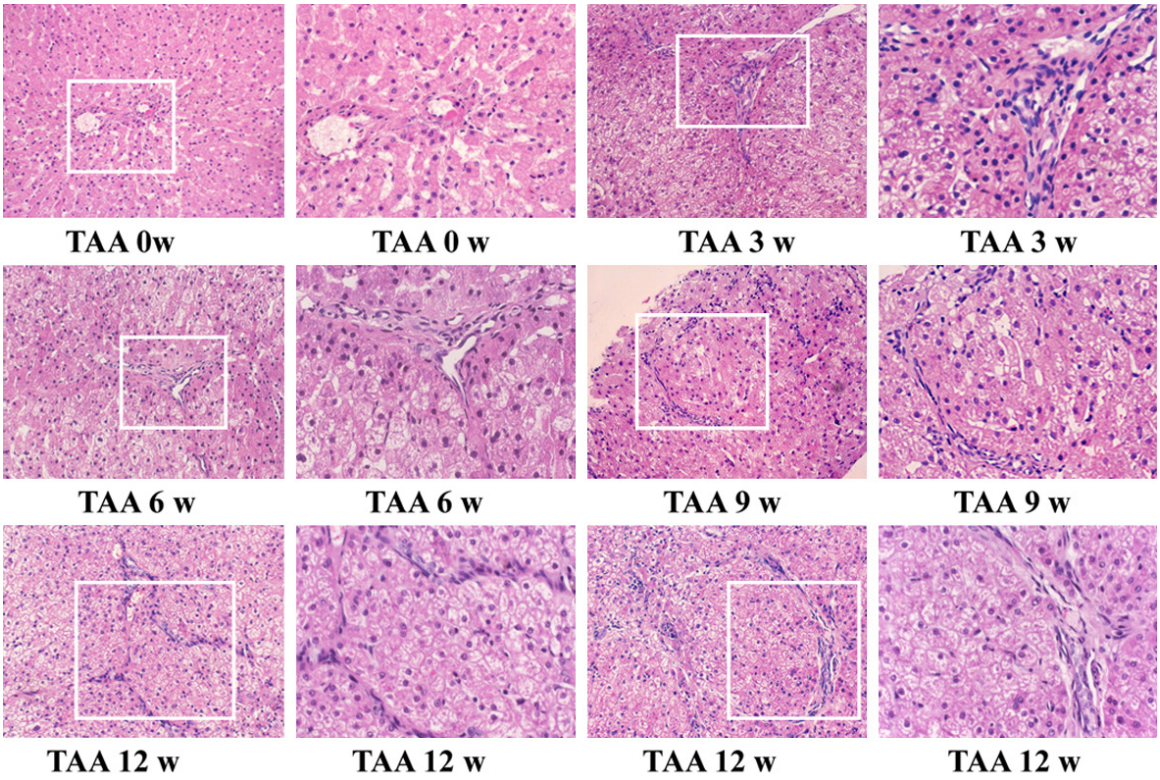

Figure S1. Pathological changes in the liver tissues of the beagles were examined at weeks 0, 3, 6, 9, and 12 after subcutaneous injection by using hematoxylin and eosin staining. Original magnification, ×200, ×400.

Table S2. Stages of hepatic fibrosis for each experimental group at 12 weeks

Groups	F0	F1	F2	F3	F4	Median
Control	6	0	0	0	0	0
IgG	6	0	0	0	0	0
TAA	0	0	0	3	3	3.5 (3, 4)[a]
TAA+rP1-Ab	0	3	3	0	0	1.5 (1, 2)[a,b]
TAA+Sil	0	2	4	0	0	2 (1,2)[a,b]

Data are presented as the median (min.-max.). Note: [a]$P < 0.05$ vs. Control group and IgG group; [b]$P < 0.05$, vs. TAA group.

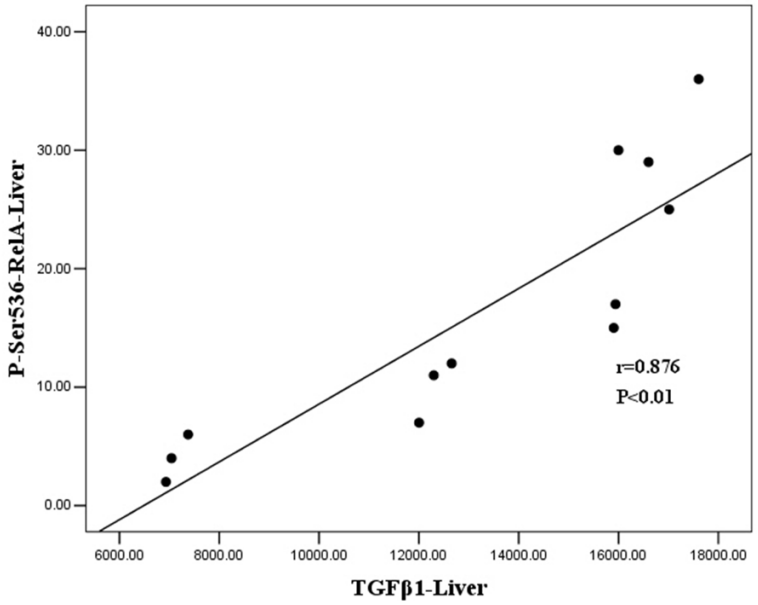

Figure S2. Relationship between the expression of TGFβ1 and P-Ser536-RelA positive cells in TAA+rP1-Ab group at multiple time points.